Direct-bandgap properties and evidence for ultraviolet lasing of hexagonal boron nitride single crystal

KENJI WATANABE*, TAKASHI TANIGUCHI AND HISAO KANDA

Advanced Materials Laboratory, National Institute for Materials Science, 1-1 Namiki, Tsukuba, 305-0044, Japan
*e-mail: WATANABE.Kenji.aml@nims.go.jp

Published online: 23 May 2004; doi:10.1038/nmat1134

The demand for compact ultraviolet laser devices is increasing, as they are essential in applications such as optical storage, photocatalysis, sterilization, ophthalmic surgery and nanosurgery. Many researchers are devoting considerable effort to finding materials with larger bandgaps than that of GaN. Here we show that hexagonal boron nitride (hBN) is a promising material for such laser devices because it has a direct bandgap in the ultraviolet region. We obtained a pure hBN single crystal under high-pressure and high-temperature conditions, which shows a dominant luminescence peak and a series of *s*-like exciton absorption bands around 215 nm, proving it to be a direct-bandgap material. Evidence for room-temperature ultraviolet lasing at 215 nm by accelerated electron excitation is provided by the enhancement and narrowing of the longitudinal mode, threshold behaviour of the excitation current dependence of the emission intensity, and a far-field pattern of the transverse mode.

Gallium nitride and related materials have been used to fabricate high-power and blue-ray laser devices[1,2], and many manufacturers now produce such devices for commercial applications. But the demand for compact ultraviolet laser devices with even shorter wavelengths seems to be increasing day by day, and this has led many researchers to search for materials with larger bandgaps than that of GaN. At present, AlN and related materials are seen as suited for ultraviolet applications. Aluminium nitride is a direct-bandgap material with a bandgap energy of about 6 eV. There are, however, many problems to be overcome (crystalline quality control, p-type conduction, and so on) before ultraviolet devices using AlN can be realized[3,4], and other materials should be thoroughly examined for this purpose.

Hexagonal boron nitride (hBN) has a wide bandgap energy. Its bandgap properties, including the bandgap energy, are not clear at present, even though the band structure has been studied experimentally[5–18] and theoretically[19–24]. Both direct and indirect properties of the bandgap have been reported, with the bandgap energies ranging from 3.6 to 7.1 eV. The properties of the band edge, and in particular whether the band edge is direct or indirect in nature, can be determined by measuring exciton-related luminescence and absorption near the edge. However, neither band-edge exciton luminescence nor absorption has so far been measurable. This seeming contradiction mainly stems from the crystalline quality of the samples used, which has been insufficient to study the intrinsic bandgap nature. Accordingly, a technique for synthesizing a pure crystalline sample is required to clarify the nature of the band edge.

A recent study of the growth of high-quality single crystals of cubic boron nitride (cBN) under high pressure and high temperature (HP/HT) has shown a Ba–B–N catalyst system to be very effective for obtaining a pure, colourless crystal[25]. By applying the Ba–B–N solvent system to hBN crystal growth under HP/HT, we have successfully obtained pure hBN single crystals. The crystal samples showed a single peak of ultraviolet luminescence at 5.765 eV (215.0 nm) at room temperature, and their intrinsic fundamental absorption spectra also had a structure from 5.822 to 5.968 eV that could be readily assigned as

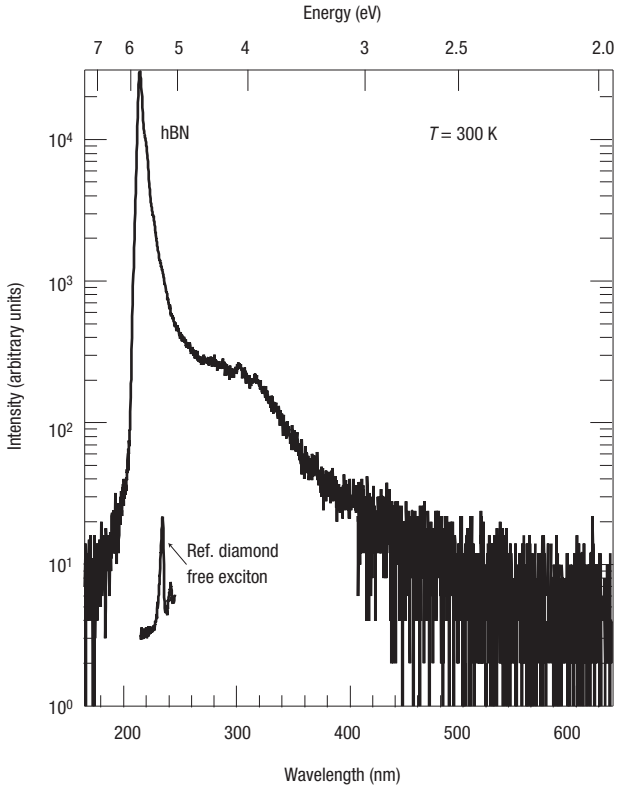

Figure 1 Example of cathodoluminescence spectrum for hexagonal boron nitride at room temperature. Indirect free exciton luminescence of pure diamond is also shown as a reference.

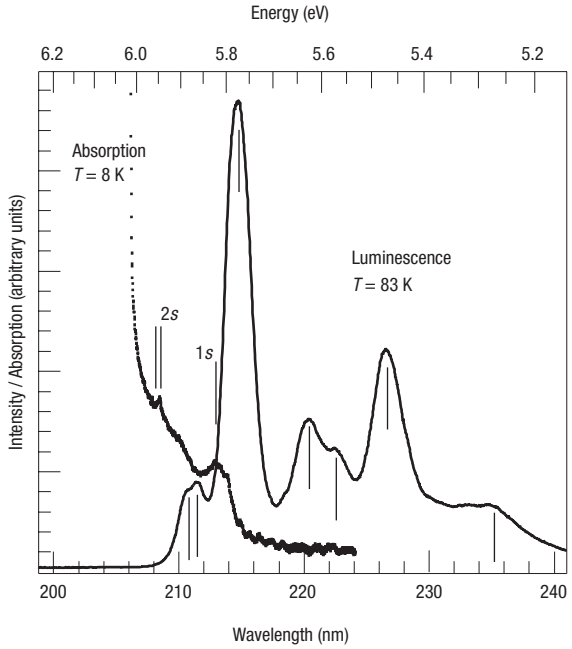

Figure 2 Fundamental absorption spectrum at 8 K and luminescence spectrum at 83 K. The weak fringes due to interference between the front and back surfaces are observed from 213 to 224 nm in the absorption spectrum. The bars indicate the peak positions for each spectrum.

an *s*-like direct exciton structure. Thus the measurements conducted on our purified crystal show that hBN is a direct-gap semiconductor with a bandgap energy of 5.971 eV. We also provide evidence for ultraviolet lasing of the crystal by accelerated electron excitation at room temperature, for which the ultraviolet luminescence band was at 215.0 nm.

An example of the cathodoluminescence spectrum at room temperature is shown in Fig. 1. A single-peaked, intense ultraviolet luminescence was observed at 5.765 eV (215.0 nm). The shoulder structures around the energy of 4 eV (300 nm), which are probably attributable to vacancies or residual impurities such as oxygen and carbon[14], are 100 times smaller than the single peak in the ultraviolet region. The contrast between the weak defect-related band and the intense ultraviolet band near band edge means that the sample has low defect density. In the case of cBN growth, contamination by oxygen is reduced by using the Ba–B–N catalyst system[25], and this impurity reduction effect is probably common to the growth of boron nitride compounds.

A spectrum of indirect exciton luminescence for diamond is also shown for comparison (Fig. 1). The peak intensity of hBN is more than 10^3 times higher than that of the indirect exciton luminescence from a type IIa pure diamond (Sumitomo Electric Industries). Note that the free exciton luminescence from diamond is so intense as to suggest that type IIa pure diamond has potential for optical device applications, although diamond is an indirect-bandgap material[26–28]. This strong emission from hBN pure crystals is evidence for the direct-gap nature of the material. That is, the band edge emission near the direct-gap energy can be intense because the conduction band minimum and valence band maximum lie at roughly the same momentum. In the effective mass approximation, the emission can be described in terms of a transfer of energy between Bloch waves of almost the same momentum near the conduction band minimum and valence band maximum, satisfying the momentum conservation rule, regardless of whether the origin of the band edge emission is impurity-related or exciton-related.

Figure 2 shows an example of a luminescence spectrum at 83 K and an absorption spectrum at 8 K; Fig. 3 shows an expanded view of part of the absorption spectrum. A series of absorption band structures of 5.822, 5.945, 5.962 and 5.968 eV (212.9, 208.5, 207.9 and 207.7 nm, respectively) was measured from the *c* plane of samples. This series of absorption bands can be readily attributed to *s*-like free exciton absorption structures between 1*s* and 4*s*, as indicated in Figs 2 and 3. In addition, the plateau known as the Elliott step[29] can be clearly seen in Fig. 3; this is the connection point between discrete exciton levels and the continuum state of band structure, and denotes the bandgap energy of direct-bandgap materials. From the minimum point of the plateau, the bandgap and the exciton binding energies are estimated as 5.971 ± 0.005 eV (207.6 nm) and 0.149 ± 0.005 eV, respectively, proving that hBN is a direct-bandgap material.

In the many theoretical papers that have been published, the calculated band structures depend on the calculation methods. Thus it is difficult to compare our experimental results with the theoretical results. Based on a work describing the symmetrical points[19], we have made a group theoretical analysis examining a dipole transition selection rule[30]. Out of the Γ, L, H, M and K points at which either valence or conduction bands show extrema in the theoretical and experimental works[5–24], we find that a direct transition polarized perpendicular to the *c* axis is allowed for the Γ ($\Gamma_5^- - \Gamma_1^+$), L ($L_1 - L_2$) and M ($M_3^+ - M_4^-$) points. This polarization direction corresponds to that for the absorption spectrum in Figs 2 and 3. Therefore, the direct gap probably lies at one of the Γ, L or M points.

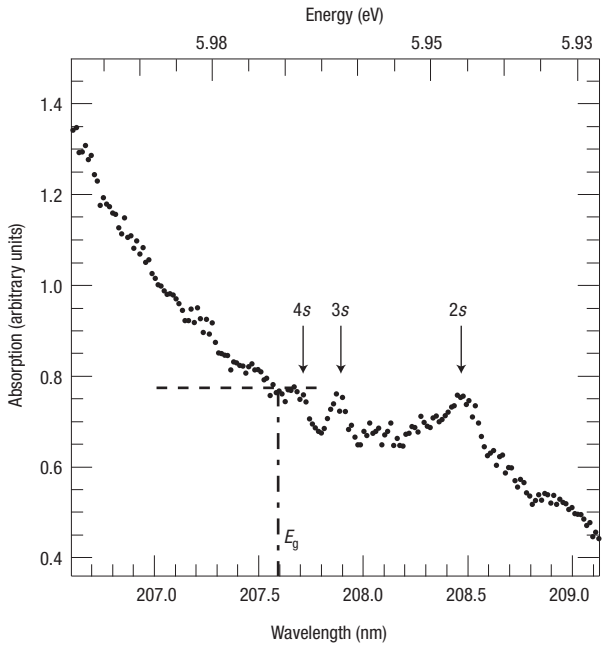

Figure 3 Expanded view of the fundamental absorption spectrum around the 2s-like exciton structure. The dashed line indicates the plateau of the Elliott step. The bandgap energy is marked as E_g.

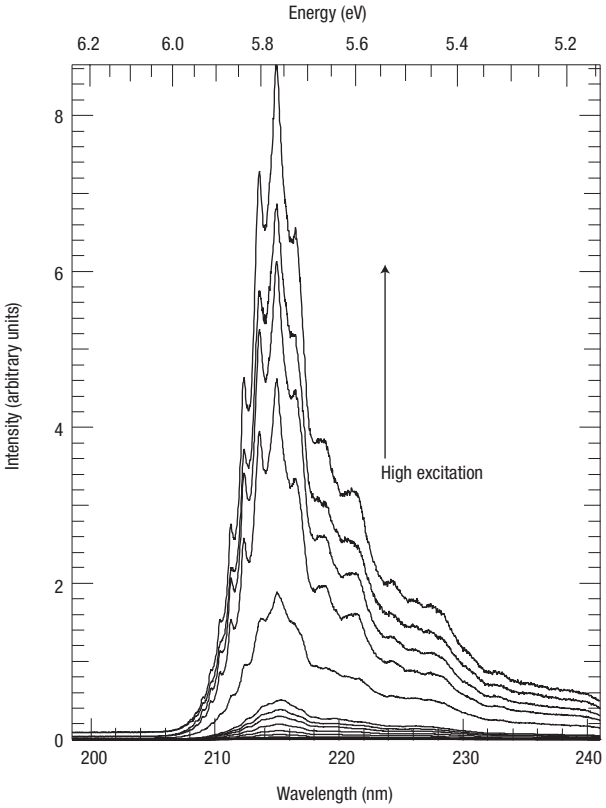

Figure 4 Excitation current dependence of the 215.0-nm luminescence band. Sharp fringe structures grow as the excitation increases. To allow comparison of weak spectra and intense ones, the excitation current was not used to normalize the spectra.

The energy difference between the 1*s* and 2*s* excitons is 0.123 eV. The corresponding exciton binding energy estimated from an atomic-hydrogen-like orbital model is 0.164 eV, which is larger than the experimentally estimated energy of 0.149 eV. This difference probably arises from the anisotropic structure of hBN. The crystal structure of hBN is composed of stacks of two-dimensional chicken-wire layers of boron and nitrogen atoms, and the interaction between the layers is much smaller than between boron and nitrogen within the layer. The nearest-neighbour distance is 0.144 nm within the chicken-wire layer, and 0.333 nm between the layers[31]. This anisotropic structure deforms the exciton wavefunction from a three-dimensional structure to quasi-two-dimensional. Using a complete two-dimensional model[32], we find that the corresponding exciton binding energy is 0.138 eV, which is smaller than the experimental value of 0.149 eV. This is reasonable, given that the exciton of hBN is expected to be described by an intermediate model between the complete two-dimensional and bulk three-dimensional structures. This partial two-dimensional confinement effect also explains why the exciton binding energy is large compared with other wide-gap materials, for example, diamond (80 meV)[33] and cubic boron nitride (80 meV; unpublished data).

Several peaks near the bandgap can be seen in the low-temperature cathodoluminescence spectrum in Fig. 2. The peak position at 5.765 eV (215.0 nm) did not show any significant energy shift from room temperature to 83 K, and the weak peaks at 5.863 eV (211.4 nm) and 5.891 eV (210.4 nm) appeared at low temperature as a result of the reduction of the width of the 215.0-nm band. The peak positions of these bands also showed no noticeable dependence on excitation current density from 0.2 to 860 mA cm^{-2}. Therefore, the origin of these bands cannot be attributed to electron–hole plasma luminescence. Note also that no electron–hole plasma luminescence[34] from the diamond reference sample can be observed with our low-current cathodoluminescence system. At present, we assume that the 5.765-eV (215.0-nm) band is the free exciton luminescence which shows a Stokes shift from the position of the 1*s* absorption peak at 5.822 eV. Similarly, both the 5.863-eV (211.4-nm) and 5.891-eV (210.4-nm) bands are assumed to be another exciton series with a Stokes shift from the energy of another exciton absorption structure, which can be weakly seen as the broad peak around 5.90 eV (210.0 nm). The origin of these Stokes shifts could be inhomogeneity of the local field near the exciton owing to impurity or dislocations such as stacking faults. The other peaks from 220 to 240 nm could be assigned as excitons bound by impurities or defects, or a phonon replica of free exciton luminescence bands.

The integrated intensity of the 215.0-nm band did not show noticeable temperature dependence from 83 to 393 K. This temperature independence arises from the huge exciton binding energy and the large radiative transition probability of the exciton, because the thermal dissociation of the exciton from 83 to 393 K is negligible compared with the exciton radiative transition rate. Thus, this temperature independence also supports the idea that hBN is a direct-bandgap material.

Figure 4 shows the spectra from a thin plate sample (about 20 μm thick) measured at room temperature while the excitation current of the cathodoluminescence system was varied. At low excitation, there seem to be weak fringes caused by the etalon effect for the cleaved surfaces of the front and back sides. As the excitation current increases, the longitudinal mode of the etalon becomes enhanced. Then the linewidth of each fringe suddenly becomes narrower above a certain excitation current. The enhancement and narrowing are attributed to stimulated emission of the luminescence band at the longitudinal mode.

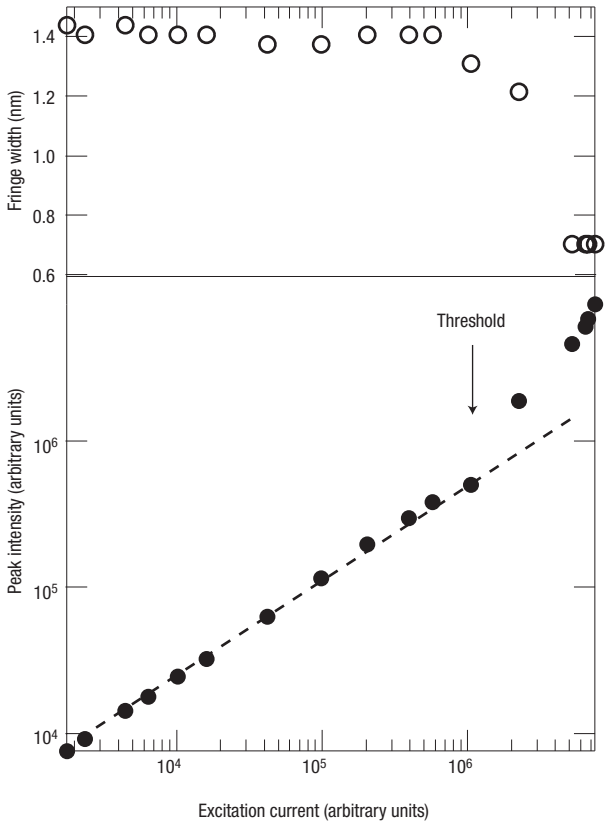

Figure 5 Excitation current dependence of the peak intensity and the fringe linewidth at 215.0 nm. The peak intensity rapidly increases and the fringe linewidth decreases from the threshold as indicated by the arrow.

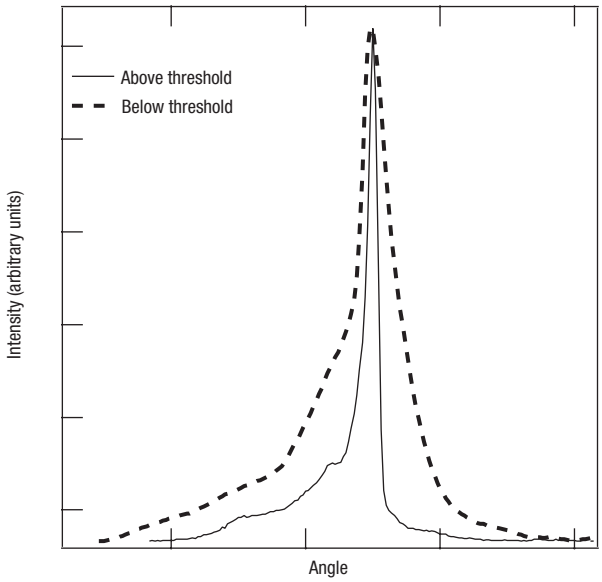

Figure 6 Change of far-field pattern for transverse mode above threshold. The dashed line is the angular distribution below the threshold and the solid line is above the threshold.

Figure 5 shows the excitation current dependence of the emission intensity and the fringe linewidth at 215 nm. The peak intensity of the emission band shows a rapid increase from the excitation current at which the enhancement of the longitudinal mode is clearly observed (arrow in Fig. 5), and the linewidth decreases rapidly around the threshold. In addition, we observed a narrowing of the far-field pattern for the transverse mode above the threshold, as shown in Fig. 6. Although we used the mirror optics of the cathodoluminescence system for this measurement, leading to complicated structure and asymmetry due to astigmatism of the collector optics, the cross-sectional angular distribution of the beam intensity clearly became narrower at excitations beyond the threshold. Together, the enhancement of the longitudinal mode, the threshold behaviour of the emission intensity, and the linewidth narrowing both for the transverse mode and for the longitudinal mode provide good evidence for the occurrence of lasing within our hBN samples.

Figures 4 and 5 were obtained from a rather rough cleaved sample which showed the threshold as described above. We have also measured the laser emission spectrum for a sample with well-cleaved surfaces, and the results are shown in Fig. 7. This sample is the same one that we examined for low-temperature absorption in Figs 2 and 3. Therefore, the fringes from 213 to 224 nm of the 8-K absorption data, caused by light transmitted through the cleaved sample, show one-to-one correspondence with the sharp fringes in Fig. 7. The fringe mode spacing is expressed by $\lambda^2/2D(n - \lambda dn/d\lambda)$, where λ, D and n denote the wavelength, the sample thickness and the index of refraction, respectively. The fringe spacing of Fig. 7 varies by a factor of 6 from 208 to 240 nm. This large change of mode spacing arises from the dispersion term $dn/d\lambda$ of the above equation. This abnormal dispersion is probably due to an exciton effect such as an exciton-polariton effect near the exciton level[35]. From this sample, we obtained an enhancement of the longitudinal mode even at a flux density of 0.2 mA cm^{-2} and an electron-beam accelerating voltage of 20 kV; thus, the threshold power of the sample is lower than 4 W cm^{-2}, which is of the same order as for optical pumping lasing for ZnO (ref. 36). This low threshold power mainly arises from the low diffraction loss of the very short cavity, and probably from excitonic gain as demonstrated in localized exciton emission of ZnSe (ref. 37).

In conclusion, several strands of evidence show that hBN is a direct-bandgap material. The intense luminescence band at 5.765 eV (215.0 nm) near the bandgap of hBN can be assigned as a direct exciton luminescence showing a Stokes shift from 5.822 eV (212.9 nm) excitonic absorption. A series of *s*-like exciton absorption bands from 1*s* to 4*s* appeared together with the plateau of the Elliott step, allowing estimates for the bandgap and exciton binding energies of 5.971 eV and 149 meV, respectively. In addition, the enhancement and narrowing of the longitudinal mode, the threshold behaviour of the excitation current dependence of the emission for the 215.0-nm band, and the change in the far-field pattern of the transverse mode indicate that the material lases when subjected to electron-beam excitation at room temperature.

Although a laser device with a p–n junction structure would require p- and n-type doping control of hBN, which remains an unsolved problem, an ultraviolet laser using hBN could readily be achieved by using an electron-beam excitation source. Such sources made from carbon nanotube, diamond and so on have recently undergone intensive investigation. Considering that hBN related materials are chemically and thermally stable, and are widely used for insulation and fireproofing, we can expect their threshold for ultraviolet damage to

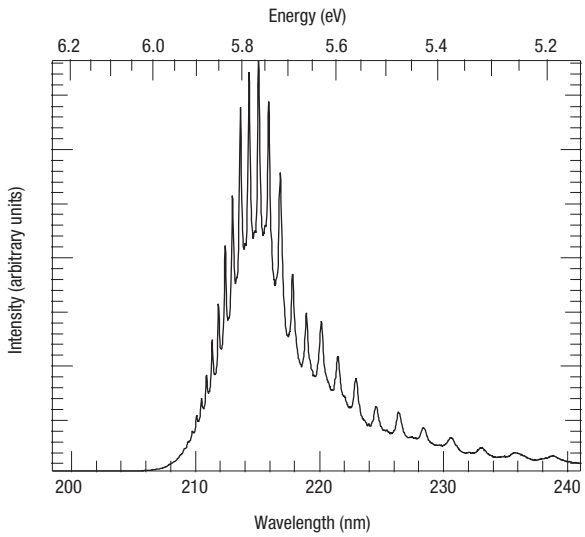

Figure 7 Example of 215.0-nm laser emission spectrum well above the excitation threshold.

be high. The ultraviolet light intensity from the samples was very stable during our experiments. This property is also promising for ultraviolet optical applications. In addition, hBN may have a variety of applications in optical devices, as its quasi-two-dimensional exciton nature should yield optical properties with large nonlinearities.

METHODS

SAMPLE PREPARATION

We used a temperature-gradient method to prepare the samples under HP/HT using barium boron nitride ($Ba_3B_2N_4$) as a solvent system. The growth cell consisted of a layered structure of Ba–B–N solvent and source of deoxidized hBN, and it was encapsulated in a molybdenum capsule. To eliminate oxygen impurities during growth, the hBN source was heat-treated at 2,000 °C in a nitrogen atmosphere. The entire process for making the growth cell was performed under a dry nitrogen atmosphere in which the O_2 and H_2O contents were kept at less than 1 part per million. The growth cell was compressed to 4.0–5.5 GPa and then heated to 1,500–1,750 °C. The holding time for the growth was varied from 20 to 80 hours. The recrystallized hBN pure crystals obtained by this method were colourless and transparent. The sample size was several cubic millimetres with a hexagonal crystalline habit. The hBN structure was confirmed by powder X-ray diffraction to have a lattice constant **c** of 0.666 nm, and our sample was of the space group $P6_3/mmc$.

CATHODOLUMINESCENCE AND FUNDAMENTAL ABSORPTION

For all the luminescence spectra, we used a cathodoluminescence spectroscopy system which consists of a scanning electron microscope (Topcon, SM350) equipped with an optical window, and mirror optics coupled to a single monochromator (Photon Design, PDP-320), and a liquid-nitrogen-cooled charge-coupled device (CCD; Roper, LN/CCD-400EB-GI). Samples were cooled from 300 to 83 K by using a liquid-nitrogen-cooled sample holder. A low-pass filter was used for taking the spectra below 400 nm, which eliminated second-order stray light from the monochromator.

The fundamental absorption spectrum was obtained from transmission experiments using a deuterium lamp as a light source. The sample was directly irradiated with ultraviolet light and the transmitted light was dispersed by a monochromator (Photon Design, PDP-320), and then detected by a liquid-nitrogen-cooled CCD (Roper, LN/CCD-400EB-GI). The sample was kept inside a helium cryostat and cooled to 8 K. The entire optical path was purged with dry nitrogen gas. The thickness of the samples ranged from 10 to 100 mm. The absorption spectrum was obtained by calculation from the direct transmission spectrum.

LASING

Cleaved samples were prepared from bulk crystal several cubic millimetres in size. A cleaved surface perpendicular to the *c* axis was easily obtained by using a sharp knife edge with a thickness ranging from 10 to 30 μm, and the Fabry–Perot etalon was composed of the front and back *c* plane. Continuous-wave excitation and detection were achieved with a cathodoluminescence system. The irradiated current of a few nanoamperes was measured with a Faraday coupler at the sample position. A smaller current was calibrated by using diamond luminescence bands[38] such as band A and H3 centre as a reference. We estimate the errors in the current-intensity measurement to be within 10% for all the measurement range. The far-field pattern of the ultraviolet light was measured by rearranging the mirror optics and the liquid-nitrogen-cooled CCD of the cathodoluminescence system. Visible stray light was eliminated by an ultraviolet narrowband filter placed in front of the CCD. All the measurements were made at room temperature.

Received 13 January 2004; accepted 13 April 2004; published 23 May 2004.

References

1. Nakamura, S. *et al.* InGaN-based multi-quantum-well-structure laser diodes. *Jpn J. Appl. Phys. Lett.* **35,** L74–L76 (1996).
2. Nakamura, S. *et al.* InGaN/GaN/AlGaN-based laser diodes with modulation-doped strained-layer superlattices grown on an epitaxially laterally overgrown GaN substrate. *Appl. Phys. Lett.* **72,** 211–213 (1998).
3. Boguslawski, P. & Bernholc, J. Doping properties of C, Si, and Ge impurities in GaN and AlN. *Phys. Rev. B* **56,** 9496–9505 (1997).
4. Onuma, T. *et al.* Exciton spectra of an AlN epitaxial film on (0001) sapphire substrate grown by low-pressure metalorganic vapor phase epitaxy. *Appl. Phys. Lett.* **81,** 652–654 (2002).
5. Zupan, J. & Kolar, D. Optical properties of graphite and boron nitride. *J. Phys. C* **5,** 3097–3100 (1972).
6. Brown, F. C., Bachrach, R. Z. & Skibowski, M. Effect of X-ray polarization at boron K edge in hexagonal BN. *Phys. Rev. B* **13,** 2633–2635 (1976).
7. Zunger, A., Katzir, A. & Halperin, A. Optical properties of hexagonal boron nitride. *Phys. Rev. B* **13,** 5560–5573 (1976).
8. Tegeler, E., Kosuch, N., Wiech, G. & Faessler, A. Electronic structure of hexagonal boron nitride. *Phys. Status Solidi B* **91,** 223–231 (1979).
9. Davies, B. M., Bassani, F., Brown, F. C. & Olson, C. G. Core excitons at the boron K edge in hexagonal BN. *Phys. Rev. B* **24,** 3537–3546 (1981).
10. Carpenter, L. G. & Kirby, P. J. The electrical resistivity of boron nitride over the temperature range 700 °C to 1400 °C. *J. Phys. D* **15,** 1143–1151 (1982).
11. Sugino, T., Tanioka, K., Kawasaki, S. & Shirafuji, J. Characterization and field emission of sulfur-doped boron nitride synthesized by plasma-assisted chemical vapor deposition. *Jpn J. Appl. Phys.* **36,** L463–L466 (1997).
12. Hoffman, D. M., Doll, G. L. & Eklund, P. C. Optical properties of pyrolytic boron nitride in the energy range 0.05–10 eV. *Phys. Rev. B* **30,** 6051–6056 (1984).
13. Tarrio, C. & Schnatterly, S. E. Interband transitions, plasmons, and dispersion in hexagonal boron nitride. *Phys. Rev. B* **40,** 7852–7859 (1989).
14. Lopatin, V. V. & Konusov, F. V. Energetic states in the boron nitride band-gap. *J. Phys. Chem. Solids* **53,** 847–854 (1992).
15. Taylor, C. A. *et al.* Observation of near band gap luminescence from boron nitride films. *Appl. Phys. Lett.* **65,** 1251–1253 (1994).
16. Jia, J. J. *et al.* Resonant inelastic X-ray scattering in hexagonal boron nitride observed by soft-X-ray fluorescence spectroscopy. *Phys. Rev. Lett.* **76,** 4054–4057 (1996).
17. Carlisle, J. A. *et al.* Band structure and core hole effects in resonant inelastic soft-X-ray scattering: Experiment and theory. *Phys. Rev. B* **59,** 7433–7445 (1999).
18. Solozhenko, V. L., Lazarenko, A. G., Petitet, J. P. & Kanaev, A. V. Bandgap energy of graphite-like hexagonal boron nitride. *J. Phys. Chem. Solids* **62,** 1331–1334 (2001).
19. Robertson, J. Electronic structure and core exciton of hexagonal boron nitride. *Phys. Rev. B* **29,** 2131–2137 (1984).
20. Catellani, A., Posternak, M., Baldereschi, A. & Freeman, A. J. Bulk and surface electronic structure of hexagonal boron nitride. *Phys. Rev. B* **36,** 6105–6111 (1987).
21. Park, K. T., Terakura, K. & Hamada, N. Band structure calculations for boron nitrides with 3 different crystal structures. *J. Phys. C* **20,** 1241–1251 (1987).
22. Xu, Y. N. & Ching, W. Y. Calculation of ground state and optical properties of boron nitrides in the hexagonal, cubic, and wurtzite structures. *Phys. Rev. B* **44,** 7787–7798 (1991).
23. Furthmuller, J., Hafner, J. & Kresse, G. Ab-initio calculation of the structural and electronic properties of carbon and boron nitride using ultrasoft pseudopotentials. *Phys. Rev. B* **50,** 15606–15622 (1994).
24. Liu, L., Feng, Y. P. & Shen, Z. X. Structural and electronic properties of h-BN. *Phys. Rev. B* **68,** 104102 (2003).
25. Taniguchi, T. & Yamaoka, S. Spontaneous nucleation of cubic boron nitride single crystal by temperature gradient method under high pressure. *J. Cryst. Growth* **222,** 549–557 (2001).
26. Kawarada, H. *et al.* Excitonic recombination radiation in undoped and boron-doped CVD diamonds. *Phys. Rev. B* **47,** 3633–3637 (1993).
27. Kawarada, H. & Yamaguchi, A. Excitonic recombination radiation as characterization of diamonds using cathodoluminescence. *Diamond Relat. Mater.* **2,** 100–105 (1993).
28. Kawarada, H., Tsutsumi, T., Hirayama, H. & Yamaguchi, A. Dominant free-exciton recombination radiation in CVD diamonds. *Appl. Phys. Lett.* **64,** 451–453 (1994).
29. Knox, R. S. *Theory of Excitons* (eds Seitz, F. & Turnbull, D.) (Academic, New York, 1963).
30. Koster, G. F. in *Solid State Physics* (eds Seitz, F. & Turnbull, D.) 173 (Academic, New York, 1957).
31. Mishima, O. & Era, K. in *Electric Refractory Materials* (ed. Kumashiro, Y.) 495–556 (Marcel Dekker, New York, 2000).
32. Shinada, M. & Sugano, S. Interband optical transitions in extremely anisotropic semiconductors. 1. Bound and unbound exciton absorption. *J. Phys. Soc. Jpn* **21,** 1936–1946 (1966).
33. Dean, P. J., Lightowlers, E. C. & Wight, D. R. Intrinsic and extrinsic recombination radiation from natural and synthetic aluminum-doped diamond. *Phys. Rev.* **140,** A352–A368 (1965).
34. Teofilov, N. *et al.* Optical high excitation of diamond: phase diagram of excitons, electron-hole liquid and electron–hole plasma. *Diamond Relat. Mater.* **12,** 636–641 (2003).

35. Masumoto, Y., Unuma, Y., Tanaka, Y. & Shionoya, S. Picosecond time of flight measurements of excitonic polariton in CuCl. *J. Phys. Soc. Jpn* **47,** 1844–1849 (1979).
36. Reynolds, D. C., Look, D. C. & Jogai, B. Optically pumped ultraviolet lasing from ZnO. *Solid State Commun.* **99,** 873–875 (1996).
37. Ding, J. *et al.* Excitonic gain and laser-emission in Znse-based quantum-wells. *Phys. Rev. Lett.* **69,** 1707–1710 (1992).
38. Zaitsev, A. M. *Optical Properties of Diamond* (Springer, New York, 2001).

Acknowledgements

We thank S. Koizumi and M. Katagiri for technical support in the lasing experiments, and T. Kuroda and K. Kobayashi for useful suggestions on the band structure of hBN.
Correspondence and requests for materials should be addressed to K.W.

Competing financial interests

The authors declare that they have no competing financial interests.